INTERNATIONAL ATOMIC ENERGY AGENCY
UNITED NATIONS EDUCATIONAL, SCIENTIFIC AND CULTURAL ORGANIZATION

INTERNATIONAL CENTRE FOR THEORETICAL PHYSICS
34100 TRIESTE (ITALY) - P.O.B. 586 - MIRAMARE - STRADA COSTIERA 11 - TELEPHONE: 2240-1
CABLE: CENTRATOM - TELEX 460392-1

SMR/390 - 4

WORKING PARTY ON "FRACTURE PHYSICS"
(29 May - 16 June 1989)

A STUDY ON THE DISLOCATION-FREE ZONE AHEAD OF THE CRACK TIP IN BULK METALLIC SINGLE CRYSTALS

K.F. HA
Department of Materials Science
Jilin University
Changchun, Jilin
People's Republic of China

A STUDY ON THE DISLOCATION-FREE ZONE AHEAD OF THE CRACK TIP IN BULK METALLIC SINGLE CRYSTALS§

K. F. Ha
(Department of Materials Science, Jilin University
Changchun, Jilin, Peoples Republic of China)

Abstract- After loading a dislocation-free zone (DFZ) was found in model I pre-cracked specimens made from different bulk single crystals (Al, Fe-3%Si, Mo). It was shown that DFZ has its own three dimensional characteristics,this conclusion was also verified by experimental facts. A new formation mechanism of DFZ was proposed, and many factors which influence the size of DFZ were discussed also.

1.INTRODUCTION

Since Kobayashi and Ohr[1] discovered the DFZ ahead of a loaded crack tip by TEM almost Ten years ago, there was still certain doubt about its existence[2]. Recently Ohr[3] repeated his experiments with thicker specimens (Fe single crystals of 1 μm in thickness) by HVEM technique, the existence of DFZ was confirmed oncemore, thus the situation seems better to him. However, 1 μm in thickness is still quite different from bulk, especially in state of stress.

From theoretical point of view both Chang and Ohr[4] and Majumdar and Burns[5] have predicted the existence of the DFZ in the case of the central crack and semi-infinite crack respectively by the method of continuous distribution of dislocations; Dai and Li [6] have also reached the same conclusion by the method ofdiscrete set of dislocations. But all of them were based on the Rice and Thomsons model[7] in which dislocations are emitted along the slip plane containing the crack front was assumed; in fact, this is not always the real case.

§ This is a lecture given in Working Party on Fracture Physics in Italy in 1989.

Besides, according to Rice and Thomsons model, the intrinsically brittle or ductile response of a material is determined primarily by whether the crack tip is stable against dislocation emission or not. Moreover, Ohr[8] pointed out in a review paper that DFZ equals zero in completely ductile materials and equals infinite in completely brittle materials. But recently Ashby and Embury[9] have made a very important suggestion that the mechanism of brittle or ductile fracture is quite independent of the stability of crack tip, it is governed by the plastic behaviour of the material to the stress field of the crack. They have shown that increase in existing dislocation density ahead of the crack tip for a given stress field causes increase in blunting by capture of dislocations during the crack propagation, and hence changes the mode of fracture.

With all these questions in mind we have performed some preliminary experiments in our laboratory. In this report some experimental results and discussions in three kinds of single crystals were presented from §2.1 to §2.3, a new experimental method in study of crack tip struture was described in §2.4, finally a brief summary of our works was addressed in §3.

2. EXPERIMENTAL RESULTS AND DISCUSSIONS

2.1 Al single crystals[10]:

The high pure (99.999%) Al single crystals used in this work were prepared by a strain-annealing method, a model I pre-crack (5 mm in length with crack tip radius about 100 μm)was introduced by spark-cutting in specimens of dimensions 30X10X2 mm as shown in Ref(11). All specimens were electric polished and then stretched to a strain about 0.2% by a SEM tensile device at room temperature, and then etched by Lacombe-Beaujard etchant[12]:

volume ratio HNO_3:HCl:HF=67:30:3.

The etching figure of undeformed specimen is shown in Fig.1, it gives an uniform dislocation density about $10^4/cm^2$.

In order to investigate the orientation dependence of DFZ, we

have stretched more than forty specimens, among them four kinds of etching figures could be chosen as representatives, they are shown in Fig.2 to Fig.5. Evidently, the so-called DFZ can be seen only in Fig.4 (DFZ of first kind) and Fig.5 (DFZ of second kind), the former is characterized by a clean or nearly clean region ahead of the crack tip, the latter is characterized by a dislocation cluster around the crack tip within the DFZ. Both in Fig.2 and Fig.3 no DFZ can be seen, but a dislocation cluster surrounds the crack tip in Fig.3.

At first, the dependence of the existence of DFZ both on the direction of crack front (the normal of the etching surface) and on the tensile direction of specimen were examined, the results are shown in Fig.6 and Fig.7 respectively. It is surprise that no rules can be found neither in Fig.6 nor in Fig.7; moreover, two different kinds of DFZ can be found at the same point in the unit triangle, for example points 5,8,17 and 9,14 in Fig.7.

In order to clarify these questions, we calculated the orientation factor (S) of all possible slip systems of different specimens and the corresponding angles α between the normal of the slip plane and the crack front. It gave us an impression that the DFZ of first kind appears only when $\alpha=90^\circ$ and the corresponding S is outstandingly large. That is the Rice and Thomson's model is satisfied rigorously, the etching figure is shown as in Fig.4. In the opposite case, when all α's are quite different from 90°, it means that crack front intersects all possible latent slip planes, and the S factor of only one slip system is the largest among all possible slip systems, no DFZ can be seen, the etching figure is shown as in Fig.2, it seems as if the external force does not feel the existence of crack in specimen. In the intermediate cases, when $\alpha\neq90^\circ$, and S factor of two slip system with different slip planes are distinctly larger than others, the etching figures are shown in Fig.3 and Fig.5. The former corresponds to α being close to 90°, and the latter corresponds to α being smaller than 90°. For example, the relevent data of specimens shown in Fig.2 to Fig.5 are listed in Table 1 to Table 4 respectively. In these tables in addition to α and S, φ and λ are the angle between tensile axis and the normal of the slip plane and the angle between tensile axis and the slip direction respectively, γ is the angle between slip line and the crack. Because the measurement of angle can not be very accurate and the Miller indices we chose are the nearest set adjoining to the real position, the error within $\pm5^\circ$ should be very satisfactory. Thus we can say that the calculated value of γ is quite in accordance with the corresponding observed value of γ, it means that the Boas-Schmid law is still valid in the bulk cracked specimens, and the appearance of the DFZ depends on both α and S.

As to the mechanism of DFZ formation, in the case of $\alpha=90^\circ$ it is just the same as described in Rice and Thomson's model. In the case of $\alpha\neq90^\circ$ dislocation can not be emitted or absorbed so easily by the crack tip as in the case of $\alpha=90^\circ$. But we can imagine that the intersecting point of the crack front and the slip plane may be a pinned point of an active dislocation spiral, so a cluster of dislocation will be formed inevitably around the crack tip. Fig.8 represents the situation of α being much smaller than 90°, it depicts the mechanism of DFZ formation of second kind in one slip system, and shows a dislocation cluster around the crack tip, it anti-shields the crack tip just as shown in Fig.5, that is also what Ohr[13] has found in TEM. Fig.9 represents the situation of α being close to 90°, it gives no DFZ but a dislocation cluster around the crack tip just as shown in Fig.3.

In short, the crack tip structure in bulk single crystals is decided by α and S simultaneously. For a given state of stretched specimen the etching figure is different for different α, so two kinds of DFZ can be found at the same point in the unit triangle as shown in Fig.7, it means that the structure of DFZ should have 3 dimensional characteristics.

As regards the unloading effect, comparing Fig.10 (DFZ of first kind) and Fig.11 (DFZ of second kind) in which (a) is in loading condition and (b) is in unloading condition, it is obvious that the unloading effect is much greater in DFZ of first kind than in DFZ

of second kind as we expected, because the net shielding effect is smaller in the DFZ of second kind. In Fig.10(b) we can find not only an obvious shrinkage in size of DFZ but a microcrack initiated at the vertex of the main crack also.

In order to investigate the formation process of DFZ, we stretched a crystal to a low stress level at first and etched, there is no trace of DFZ; then stretched again to a high stress level and etched, the figure of DFZ was presented. It means that the DFZ was formed after a critical deformation. The same problem was studied quantitatively with Fe-3%Si single crystal in next section.

2.2 Fe-3%Si single crystals[14]:

All single crystals used in this investigation were cut from Fe-3%Si steel plate with coarse grained Gaussian texture $\{110\}\langle 001\rangle$ into 40X10X3mm in dimensions, model I pre-crack(3, 3.5 and 4 mm in length with crack tip radius about 100 μm) in [001] direction was introduced by spark-cutting also. Since the observation surface was always (110), for slip plane $(\bar{1}12)$ $\alpha=90^{\circ}$, its corresponding S= 0.47 which is the largest one among all possible slip system, the relevent data are listed in Table 5. According to the analysis given in last section, DFZ of first kind should be formed. Fig.12 (a),(b) and (c) are the experimental results in which (a) is the undeformed state, the dislocation density is about $4X10^4$/cm, (b) corresponds to a strain of 1.9%, (c) corresponds to a strain of 1.5%. All etching figures were obtained by the following sequential processes:

Electric polishing⟶Deformation⟶aging⟶Electric polishing ⟶Etching.

The etching solution used was:

25g CrO_3 + 133ml CHCOOH + 7ml H_2O[15,16].

Since the rolling plane can never be the exact (110) plane in each grain for Gaussian texture, two sets of slip lines were revealed and identified as $(\bar{1}12)[1\bar{1}1]$ and $(1\bar{1}2)[\bar{1}11]$ correspondingly, and the latter is exactly equivalent to the former.

Comparing (b) and (c) in Fig.12, it is evident that the size of

DFZ is larger in high strained specimen. Because there is still no theoretical relation to predicate the dependence of the size of DFZ on externally applied load, we measured the size variation of DFZ in specimens with different length of pre-crack against applied load experimentally. The results are shown in Fig.13, they can be expressed by the following analytical expression

$$D(X500)\ cm=Kc(e^{P/P_0-1}-1)$$

where D is the width of DFZ along the crack direction, K is a simulative constant, c is the pre-crack length in cm, P is the externally applied load, P_0 is that corresponding to the initiation of DFZ, it equals 45 kg, 44 kg and 34 kg when c=0.3 cm, 0.35 cm and 0.4 cm respectively, for a best fit K was chosen to be 11.7 . From Fig.13 it shows that the size of DFZ increases monotonously with increase in applied load and such tendency becomes stronger after $c>0.35$ cm.

In order to study the influence of sharpness of the pre-crack on the DFZ formation, specimen which had been hydrogen cracked before deformation showed well defined DFZ ahead of each microcrack tip after stretch (to a strain of 2.3%). Fig.14(a) is the general view of a large area of the specimen, Fig.14(b) is an enlarged view of a microcrack in the lower right part of Fig.14(a). The size of DFZ ahead of each microcrack is much smaller than that ahead of the main crack evidently.

In order to study the influence of pinning effect of dislocation on the DFZ formation, specimen which had been decarbonized and denitrided for 72 h before deformation showed no DFZ after stretching to the same degree (2.3%). It means that the activation of dislocation sources in lattice is unfavorable to the DFZ formation , the result is shown in Fig.15. If the specimen had been treated by decarbonization and denitrogenation at first, we repeated the foregoing hydrogen cracking process, there was no DFZ ahead of any microcrack after stretch, the result is shown in Fig.16.

2.3 Mo single crystals:

The Mo single crystal was made by electron beam floating method as described in Ref(17). Specimens used in this work were thin plates of 10X6X1 mm in dimensions with T shoulders, a model I precrack (3mm in length with crack tip radius about 100 μm) was introduced by spark-cutting along [110] direction. The observation surface was (111), the etching solution for this surface was:

volume ratio $CH_3OH:H_2SO_4:HCl=30:6:13$.

Fig.17 is a typical DFZ of second kind after stretching to a strain of 0.1%, the striking feature is that the substructure formed during crystal preparation was still remained in its original form. The same result was obtained also in mode III loading.

2.4 A new experimental method in study of DFZ:

Since X-ray can penetrate a certain depth into the specimen, a pseudo Kossel photographical method was chosen to study the inner structure of the crack tip. This method gave a back reflection pattern from a fine focussed divergent beam X-ray source, Fig.18 is a pseudo Kossel figure of an undeformed Al single crystal specimen. With the same specimen we deformed it to a strain of 0.2%, it gave a DFZ of first kind as shown in Fig.19. We adjusted the irradiated area to coincide with the boundary region between the DFZ and the plastic zone, then a pseudo Kossel pattern was obtained as shown in Fig.20. In Fig.18 the sharpness of each diffraction line is homogeneous except a little geometrical broadening in the distance, but in Fig.20 the sharpness of each diffraction line is seriously inhomogeneous. It is evident that in Fig.20 the broadened part of diffraction lines was given by the deformed lattice in the plastic zone, the sharpened part of diffraction lines was given by the lattice in DFZ. Moreover, Fig.21 is the pseudo Kessel pattern given by the crack tip in Fig.2 which shows no DFZ by etching, but it is quite similar to Fig.20.

Similar conclusion was obtained in Mo single crystals also, Fig. 22 and Fig.23 are the pseudo Kossel patterns of undeformed and deformed specimens respectively, they are very similar to Fig.18 and Fig.20 in Al single crystals. Therefore, the three dimensional characteristics of DFZ is proved by the pseudo Kossel photographical method.

3. SUMMARY

Up to now either from theoretical point of view or from the experimental facts we should have no doubt about the existence of a DFZ ahead of a loaded crack. It gives not only an explanation to the so-called Rice Paradox but a new enlightenment in study of crack tip structure. In this report we have verified that such DFZ may spread itself in three dimensions around the crack front in a bulk single crystal, and its appearance may be influenced by many factors, for example crystal orientation, length and sharpness of the crack, pinning condition of dislocations in lattice, applied load and the method in crystal preparation etc. But we are still obscure to the real mechanism of DFZ formation, such as how can the fundamental structures of a real crystal disappear within the DFZ and the formation dynamics of such DFZ.

As to the influence of DFZ on the mechanical properties of $\overset{a}{\lambda}$ cracked crystal, there are still many aspects needed to discuss. From the current point of view it seems as if a competition exists between the dislocation emission and cleavage, when a crack is subject to an applied load. The intrinsically ductile or brittle response of material is determined by the stability of the crack against dislocation emission. But in fact detailed experimental observations have shown conclusively that dislocation emission occurs not only from stationary but from propagating cleavage cracks (1,18-21). In addition, we must point out that in general it is more favorable to emit dislocations from crack tip when $\alpha=90^\circ$, but there are still two advantages in dislocation emission when $\alpha\neq 90^\circ$. One is that it is possible that dislocation spiral may operate continuously without the need of repeatedly nucleating dislocation loop as in the Rice-Thomson's model, the other is that emitting dislocations in this way will not lower the crack tip stress intensity factor so serious as that in Rice-Thomson's model also. Therefore emitting dislocations from a propagating cleavage crack may be performed in a great variety of ways.

Besides the foregoing geometrical consideration there is a physical condition which is favorable to emit dislocations from a propagating cleavage crack. According to the dynamic consideration of Johl, Kameda, McMahon Jr and Vitek[22] also the atom-pair separation must reach a critical distance when breaking of the bond takes place eventually in cleavage process, It means that a certain period must be spent to reach this critical distance, so during the same time dislocation emission can take place until the crack tip tensile stress is lowered to a minimum value by which cleavage can continue no longer as before. Therefore dislocation emission from a propagating cleavage crack is absolutely possible in physics.

Finally, I believe that in addition to what we have discussed dislocation density ahead of the crack tip, the mobility of these dislocations and the velocity of the crack concerned etc all of these will decide the cleavability of the crack with great complexity, so it would be better to do some critical experiments before any theoretical analysis is taken.

ACKNOWLEDGEMENTS

This work was supported by the National Natural Science Foundation of China under contract No. 5860322.

REFERENCES

1. S. Kobayashi and S. M. Ohr, Phil. Mag. A42, 763 (1980).
2. I. Robertson and H. K. Birnbaum, II Int. Conf. Fundamentals of Fract., Gatlinburg, TN. (1985).
3. S. M. Ohr, Phil. Mag. A57, 677 (1988).
4. S. J. Chang and S. M. Ohr, J. Appl. Phys. 52, 7174 (1981).
5. B. S. Majumdar and S. J. Burns, Int. Journ. of Fracture 21, 229 (1983).
6. S. H. Dai and J. C. M. Li, Scripta Met. 16,183 (1982).
7. J. R. Rice and R. Thomson, Phil. Mag. 29, 73 (1974).
8. S. M. Ohr, Materials Science and Engineering 72, 1 (1985).
9. M. Ashby and J. Embury, Scripta Met. 19, 557 (1985).

10. J. Li, X. H. Wang, Y. B. Xu and K. F. Ha , to be published.
11. X. H. Wang, Y. B. Xu, G. Z. Wang and K. F. Ha, Phys. Stat. Sol. (a) 104, K79 (1987).
12. W. Schatt and I. Garz, Prakt. Metall. 4, 574 (1967).
13. S. M. Ohr, Scripta Met. 21, 1681 (1987).
14. C. S. Yang, X. H. Wang, Y. B. Xu and K. F. Ha,to be published.
15. C. G. Dunn and F. W. Daniels, Trans. AIME, 191, 147 (1951).
16. C. E. Morris, Metal Progr. 65, 696 (1949).
17. K. F. Ha and Z. Z. An, J.Appl. Phys. 55, 94 (1984).
18. J. M. Liu and B. W. Shen, Metall. Trans. 15A, 1247 (1983); 15A, 1253 (1983).
19. C. st. John, Phil.Mag. 32, 1193 (1975).
20. S. J. Burns and W. W. Webb, J. Appl. Phys. 29, 600 (1958).
21. S. J. Burns, Acta Met. 18, 969 (1970).
22. M. L. Jokl, Jun Kameda, C. J. McMahon Jr. and V. Vitek, Metal Science 14, 375 (1980).

TABLES AND FIGURE CAPTIONS

Table I. Data of Fig.2
Surface of observation (102)
Tensile direction [22$\bar{1}$]

Slip surface	α°	φ°	$\gamma_{cal.}$	Slip direction	λ°	S	$\gamma_{obs.}$
111	39	55	23	$\bar{1}10$	90	0	28
				$10\bar{1}$	46	0.40	
				$01\bar{1}$	46	0.40	
$1\bar{1}1$	39	80		011	76	0.04	
				110	19	0.16	
				$10\bar{1}$	46	0.12	
$\bar{1}11$	77	80		110	19	0.16	
				101	76	0.04	
				$01\bar{1}$	46	0.12	
$11\bar{1}$	77	16		011	76	0.23	
				$\bar{1}10$	90	0	
				101	76	0.23	

Table II. Data of Fig.3
Surface of observation (320)
Tensile direction [$\bar{2}3\bar{1}$]

Slip surface	α°	φ°	γ_{cal}	Slip direction	λ°	S	
111	37	90		$\bar{1}10$	19	0	
				$10\bar{1}$	78	0	
				$01\bar{1}$	44	0	
$1\bar{1}1$	82	21	20	011	63	0.42	
				110	76	0.22	
				$10\bar{1}$	78	0.19	
$\bar{1}11$	82	54	51	110	76	0.11	
				101	57	0.31	
				$01\bar{1}$	44	0.42	+
$11\bar{1}$	37	72		011	63	0.14	
				$\bar{1}10$	19	0.29	
				101	57	0.17	

+ No slip lines observed.

Table III. Data of Fig.4
Surface of observation $(\bar{1}34)$
Tensile direction $[01\bar{1}]$

ip ace	α°	φ°	$\gamma^\circ_{cal.}$	Slip direction	λ°	S	$\gamma^\circ_{obs.}$
1	47	90		$\bar{1}10$	60	0	
				$10\bar{1}$	60	0	
				$01\bar{1}$	0	0	
1	90	35	34	011	90	0	
				110	60	0.41	25
				$10\bar{1}$	60	0.41	
1	25	90		110	60	0	
				101	60	0	
				$01\bar{1}$	0	0	
$\bar{1}$	77	35		011	90	0	
				$\bar{1}10$	60	0.41	
				101	60	0.41	

Table IV. Data of Fig.5
Surface of observation (013)
Tensile direction $[3\bar{1}0]$

Slip surface	α°	φ°	$\gamma^\circ_{cal.}$	Slip direction	λ°	S	$\gamma^\circ_{obs.}$
111	43	43	15	$\bar{1}10$	64	0.32	13
				$10\bar{1}$	47	0.49	
				$01\bar{1}$	77	0.16	
$1\bar{1}1$	69	68		011	77	0.08	
				110	27	0.33	
				$10\bar{1}$	47	0.25	
$\bar{1}11$	43	68		110	27	0.33	
				101	47	0.25	
				$01\bar{1}$	77	0.08	
$11\bar{1}$	69	43	34	011	77	0.16	+
				$\bar{1}10$	64	0.32	
				101	47	0.49	

+ No slip lines observed.

Table V. Data of Fig.12
Surface of observation (110)
Tensile direction $[1\bar{1}0]$

Slip surface	α°	φ°	$\gamma^\circ_{cal.}$	Slip direction	λ°	S	$\gamma^\circ_{obs.}$
112	55	90		$11\bar{1}$	90	0	
$\bar{1}12$	90	55	55	$1\bar{1}1$	35	0.47	52
121	30	75		$1\bar{1}1$	35	0.21	
$\bar{1}21$	75	30		$\bar{1}\bar{1}1$	90	0	

Fig.1 Original state ahead of the crack tip of Al single crystal.(SEM)
Fig.2 No DFZ, no dislocation cluster ahead of the crack tip of stretched Al single crystal.
Fig.3 No DFZ, but dislocation cluster ahead of the crack tip of stretched Al single crystal. (SEM)
Fig.4 DFZ of first kind ahead of the crack tip of stretched Al single crystal. (SEM)
Fig.5 DFZ of second kind ahead of the crack tip of stretched Al single crystal. (SEM)
Fig.6 Dependence of the existence of DFZ on the direction of crack front.

Fig.7 Dependence of the existence of DFZ on the tensile direction.
Fig.8 Mechanism of DFZ formation of second kind in one slip system.
Fig.9 Mechanism of formation of some dislocation cluster around the crack tip but no DFZ.
Fig.10 (a) is DFZ of first kind under loading condition in Al single crystal, (b) is the same specimen after unloading.
Fig.11 (a) is DFZ of second kind under loading condition in Al single crystal, (b) is the same specimen after unloading.
Fig.12(a) Original state ahead of the crack tip of Fe-3%Si single crystal.
Fig.12(b) DFZ after stretching to a strain of 1.9% in Fe-3%Si single crystal. (SEM)
Fig.12(c) DFZ after stretching to a strain of 1.5% in Fe-3%Si single crystal. (SEM)
Fig.13 Dependence of the size of DFZ on crack length and applied load in Fe-3%Si single crystal.
Fig.14(a) DFZ ahead of microcrack tips in hydrogen charged Fe-3%Si single crystal.
Fig.14(b) An enlarged view of a microcrack tip in the lower right part of Fig.14(a). (SEM)
Fig.15 Crack tip in Decarbonized and denitrided Fe-3%Si single crystal after stretch. (SEM)
Fig.16 No DFZ is found ahead of any microcrack tip after stretching a hydrogen charged decarbonized and denitrided Fe-3%Si single crystal.
Fig.17 DFZ of second kind in stretched Mo single crystal with model I pre-crack.
Fig.18 A pseudo Kossel pattern of an undeformed Al single crystal.
Fig.19 DFZ of first kind in stretched Al single crystal with model I pre-crack.
Fig.20 A pseudo Kossel pattern given by the region across the DFZ and the plastic zone as shown in Fig.19.
Fig.21 A pseudo Kossel pattern given by the crack tip in Fig.2.
Fig.22 A pseudo Kossel pattern given by the undeformed Mo single crystal.
Fig.23 A pseudo Kossel pattern given by a stretched Mo single crystal with model I pre-crack.

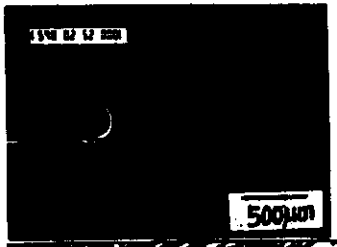

Fig.1 Original state ahead of the crack tip of Al single crystal. (SEM)

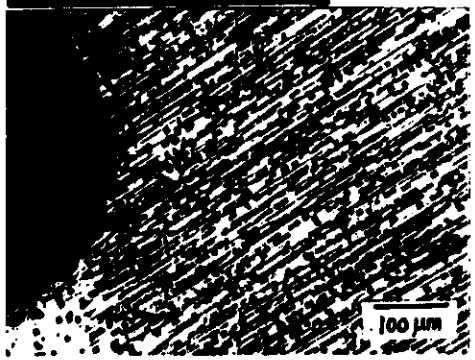

Fig.2 No DFZ, no dislocation cluster ahead of the crack tip of stretched Al single crystal.

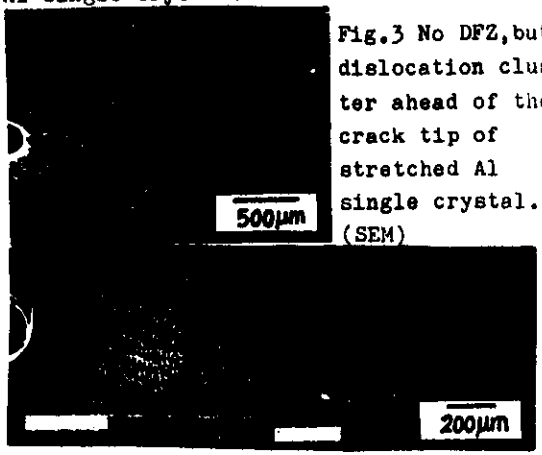

Fig.3 No DFZ, but dislocation cluster ahead of the crack tip of stretched Al single crystal. (SEM)

Fig.4 DFZ of first kind ahead of the crack tip of stretched Al single crystal. (SEM)

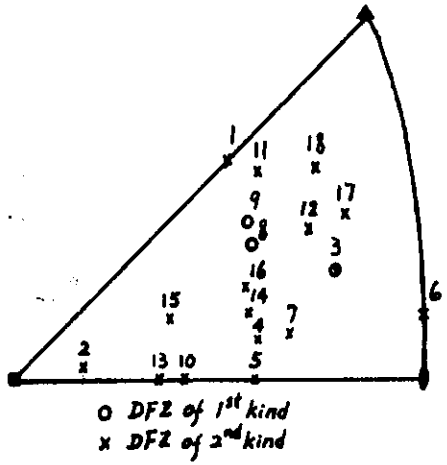

Fig.6 Dependence of the existence of DFZ on the direction of crack front.

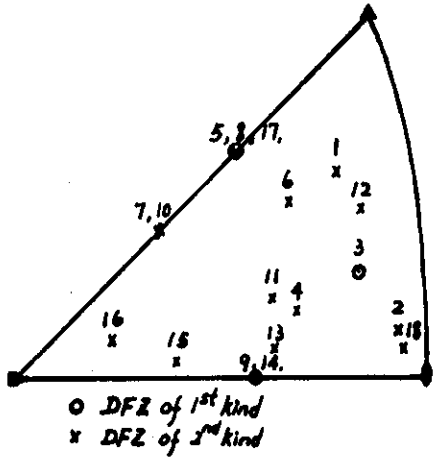

Fig.7 Dependence of the existence of DFZ on the tensile direction.

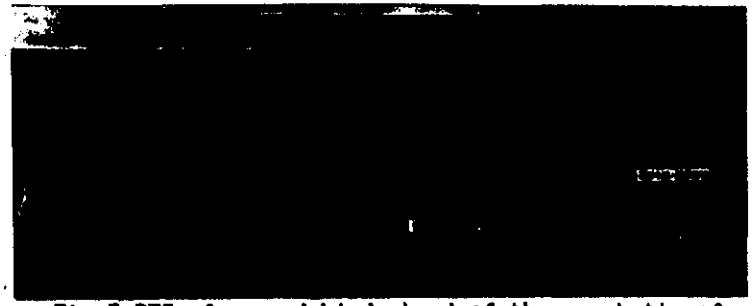

Fig.5 DFZ of second kind ahead of the crack tip of stretched Al single crystal. (SEM)

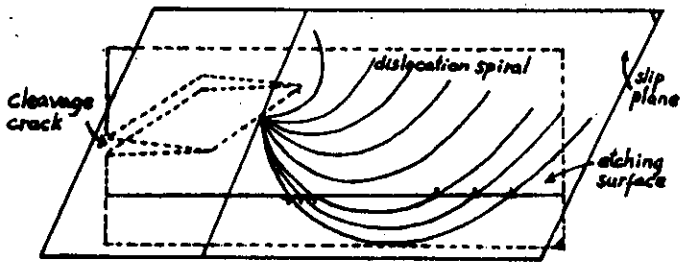

Fig.8 Mechanism of DFZ formation of second kind in one slip system.

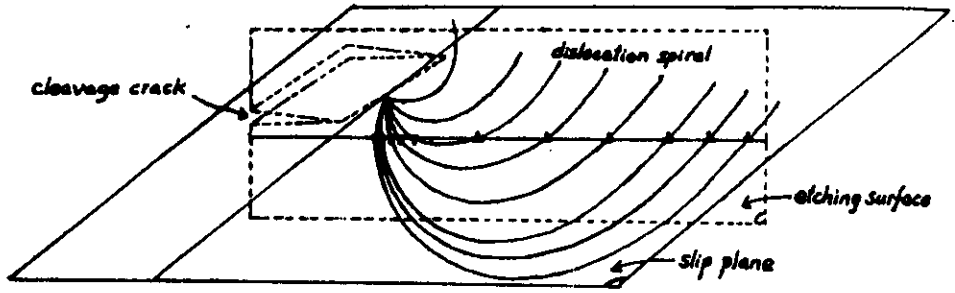

Fig.9 Mechanism of formation of some dislocation cluster around the crack tip but no DFZ.

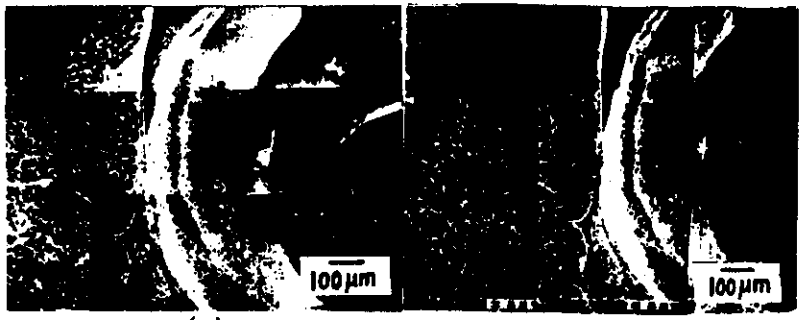

(a) (SEM) (b)

Fig.10(a) is in loading condition of DFZ of first kind in Al single crystal, (b) is after unloading of the same specimen.

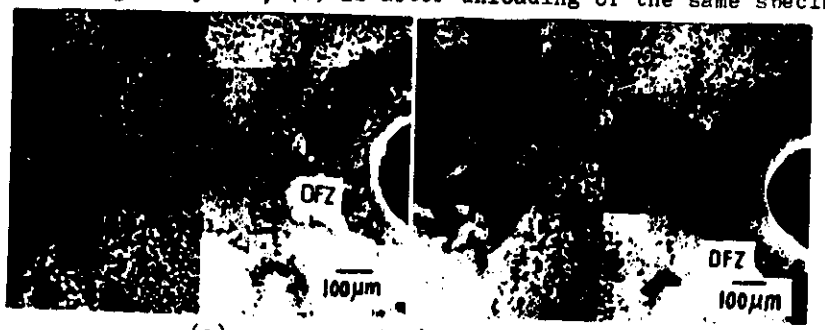

(a) (SEM) (b)

Fig.11(a) is in loading condition of DFZ of second kind in Al single crystal, (b) is after unloading of the same specimen.

Fig.12(a) Original state ahead of the crack tip of Fe-3%Si single crystal.

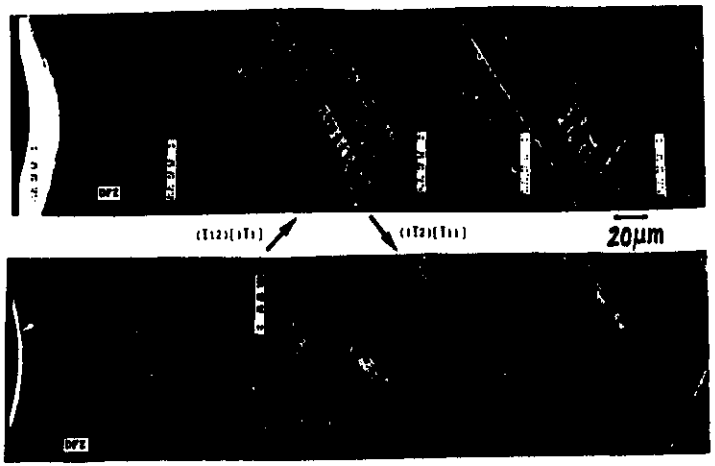

(b)

(c)

Fig.12(b) DFZ after stretching to a strain of 1.9% in Fe-3%Si single crystal. (SEM)

Fig.12(c) DFZ after stretching to a strain of 1.5% in Fe-3%Si single crystal. (SEM)

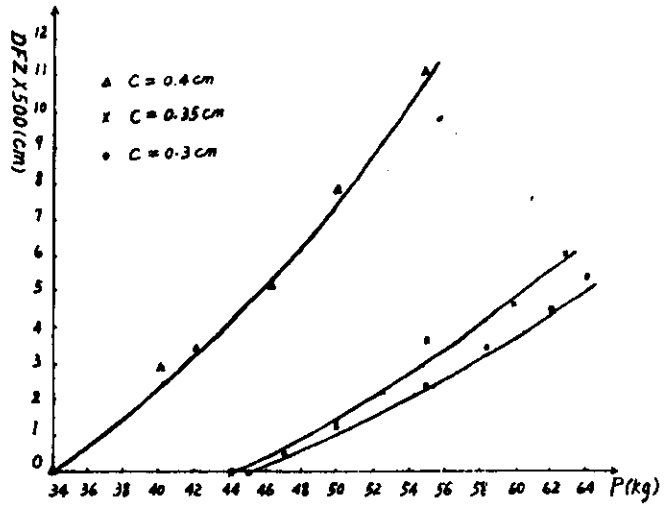

Fig.13 Dependence of the size of DFZ on crack length and applied load in Fe-3%Si single crystal.

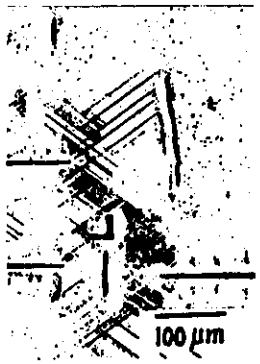

(a)

Fig.14(a) DFZ ahead of microcrack tips in hydrogen charged Fe-3%Si single crystal.

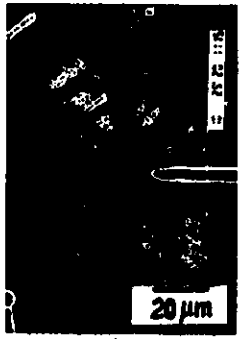

(b)

Fig.14(b) An enlarged view of a microcrack tip in the lower right part of Fig.14 (a). (SEM)

Fig.15 Crack tip in decarbonized and denitrided Fe-3%Si single crystal after stretch. (SEM)

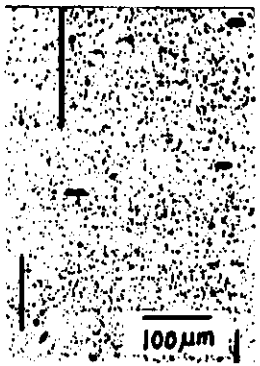

Fig.16 No DFZ is found ahead of any microcrack tip after stretching a hydrogen charged decarbonized and denitrided Fe-3%Si single crystal.

Fig.17 DFZ of second kind in stretched Mo single crystal with model I pre-crack.

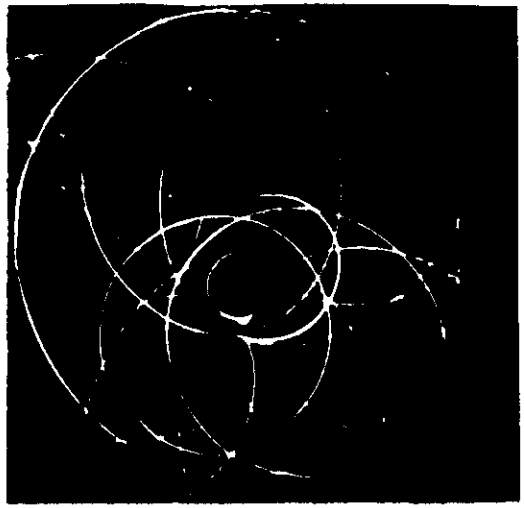

Fig.18 A pseudo Kossel pattern of an undeformed Al single crystal.

Fig.19 DFZ of first kind in stretched Al single crystal with model I pre-crack.

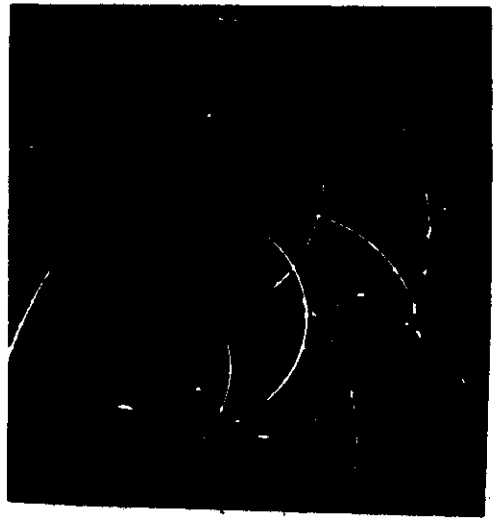

Fig.20 A pseudo Kossel pattern given by the region across the DFZ and the plastic zone as shown in Fig.19.

Fig.21 A pseudo Kossel pattern given by the crack tip in Fig.2.

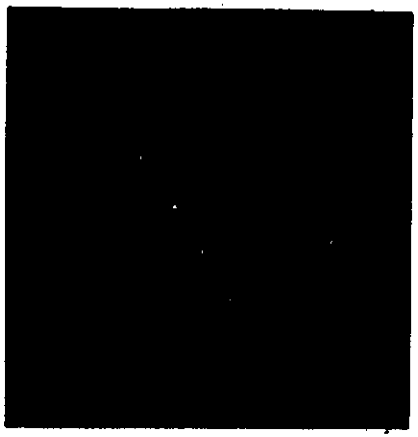

Fig.22 A pseudo Kossel pattern given by the undeformed Mo single crystal.

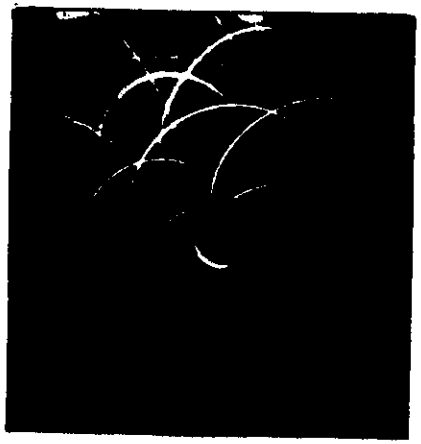

Fig.23 A pseudo Kossel pattern given by a stretched Mo single crystal with model I pre-crack.